MODELING SUPRAGLACIAL LAKE DRAINAGE AND ITS EFFECTS ON THE SEASONAL EVOLUTION OF THE SUBGLACIAL DRAINAGE SYSTEM IN A TRIBUTARY GLACIER SETTING

By

Nevil Arley Franco, B.Sc., A.A.

A Thesis Submitted in Partial Fulfillment of the Requirements

for the Degree of

Masters of Science

in

Physics

University of Alaska Fairbanks

August 2021

APPROVED:

Dr. Martin Truffer, Committee Chair
Dr. Renate Wackerbauer, Committee Member
Dr. Peter Delamere, Committee Member
Dr. Martin Truffer, Chair
Department of Physics
Dr. Kinchel Doerner, Dean
College of Natural Science & Mathematics
Dr. Richard Collins,
Director of the Graduate School

Abstract

This work aims to gain a better understanding of the relationship between glacier motion and water distributed through subglacial drainage systems. A numerical scheme (GlaDS) is used to model both inefficient and efficient drainage systems to see which dominates after the draining of a supraglacial lake on a synthetic glacier that is made up of an outline that features a main branch and a tributary. The geometry is based on the surge-type Black Rapids Glacier (Ahtna Athabascan name: Dału'itsaa'den) in Alaska, where a lake develops in the higher ablation zone, and drains rapidly early in the melt season. It has also been observed that this lake drainage causes a twofold or threefold speed-up of the main branch, with some acceleration of the lower-lying Loket tributary. This speed-up can be considered a surrogate for a surge, which also initiates in the main branch, while, during times of quiescence, the ice flow on the tributary is dominant. We investigate the effects of varying timing and volume inputs of lake drainage with a focus on its effects beneath the tributary. We find that the response of the glacier depends on the seasonal timing, the amount of water from the draining lake, and its location on or near the margins of the glacier. Results show that an inefficient drainage system is the cause of the glacier speed-up, both when the lake drains rapidly or when there is an extended time in drainage, at any time of the season. The speed signals vary throughout the glacier depending on the location of the lake relative to that of an evolved efficient drainage system.

Table of Contents

List of Figures

Acknowledgments

First and foremost, me gustaría agradecer a mi querido asesor, un gigante en glaciología, mi Profesor Jirafales, Dr. Martin Truffer. I did not know a thing about glaciers and knew very little about coding when I went to you to inquire about a thesis project. I am very grateful that you took me under your tutelage, guiding me through the perils of coding, and showing me how to thoroughly think through the physics of complex systems. Your recurring laughing and unrestrained, but uncommon, cursing made it comfortable for me to be myself which helps a lot. Thank you for the flying opportunities that took us over glaciers and to touch down on Black Rapids Glacier!

I would like to thank my other committee members, Drs. Renate Wackerbauer and Peter Delamere, for their help in drafting this thesis and for teaching some of the best physics courses I have ever taken. As a dedicated future educator, your ways of teaching will be carried on! This sentiment also applies to Dr. David Newman, who also shared the importance of physics education and what we can learn from studies that help us teach physics through effective ways. Thank you for being the physics guide of Alaska. (I think I saw a green flash!) Thank you Dr. Mauro Werder for the use of the GlaDS model; it was a challenge learning to use it but I did learn a lot from going through it.

I would like to thank my persistent physics cohort. Cameron, we didn't spend a whole lot of time together, but the times we did hang out were great because there was always a great conversation to be had. Zak, it was great having you as a fellow grad student and as a supervisor/mentor in the labs. I also appreciate the constant pushing and nudging to consider teaching as a career, it'll definitely happen! Dempsey, thanks for having my back in the corners we found ourselves in, from the courses we took to the Alaskan dry cabin life. Our night walks back to the cabins (and our detours) in the woods when it was thirty below are great memories. Our one-on-one conversations in days of uncertainty and frustration were great stress relievers and getting new perspectives on life.

Thank you to the Weston bubble (Ems, David, Lynn, Valerie, Liam, and Hannah) for breaking my pandemic solidarity, especially when things got emotionally tough. The generosity, the Kombio sessions (I'll remember the rules one day!), and the friendship will be cherished forever. It was great to get to meet wonderful people at the Geophysical Institute (too long of list of names that I'll probably forget some people, but you know who you are!), especially those in the glaciers group (Chris, Joanna, Emilie, Andrew, Jenna, Eric, Maria, Victor, and Kyle). I would like to thank those that I have stayed in touch with even after we went very separate ways, it's good to know that friendships can last even our lives unfolding before us.

Dedications

This work is dedicated to my parents, Maria Soledad Franco and Carlos Alfonso Franco. Thank you for your undying love and support. And also to my uncle Cesar Augusto Samayoa, que descanse en paz.

1.0 Introduction

Glaciers experience an increase in ice flow velocity during the warmer part of the year, often referred to as "spring events" or "mini-surges"(Willis, 1995). Around this time, melt on the surface is enhanced and the meltwater drains to the bed, lubricating the interface between the ice and bed, allowing the glacier to accelerate. Surface velocities increase 2-10 fold in events that last between a few hours to several days and then go back to background speeds. All glaciers are known to flow at a relative constant rate due to gravitational stress brought on by their mass, but there are certain glaciers that experience a unique phenomena known as *surging*.

Surging is a quasi-periodic speed-up and displacement of ice that has reached a critical accumulative thickness in an area known as the *reservoir zone*. This causes an instability in the flow where the ice moves towards the *receiving zone* that is located at the lower part of the glacier and can extend beyond the glacier boundary. This transport of mass thins out the glacier in the reservoir zone and thickens the receiving zone. This event can last months to decades, eventually coming to a quiescent phase (Cuffey and Paterson, 2010). Surging glaciers have a complex relationship with environmental factors, so the onset of surging is still not well understood (Benn and others, 2019), and only a small fraction ($\sim$1%) of the glaciers worldwide (Sevestre and Benn, 2015) experience this event.

Observations (Hewitt, 2007; Paul and others, 2017) have shown that surges are more common in glaciers that have *tributaries*, smaller glaciers flowing into the larger main branch. During a surge, the main branch advances, but a tributary can slow down and be sheared off by the fast flowing ice. When surging stops, the tributary regains its flow speed before the surge. Evidence that this type of event has occurred can be seen from debris on the surface in the form of *moraines*, a collection of rock and soil that has been deposited from sidewall erosion transported down-glacier. Tributaries also carry these moraines, but when they merge into the main branch, the debris coalesces into medial moraines (Fig 1.1).

Other observations on surging glaciers show some common features (Harrison and Post, 2003) such as having a soft bed of variable thickness made of *till* (granular, deformable, micro-porous substrate) and/or meltwater draining into a seasonal-dependent subglacial drainage system. This work will focus on modeling the latter since it is difficult to observe subglacial hydraulics directly. The mechanics behind how water flows subglacially is an open question, but extensive field experiments (i.e. borehole measurements of water pressures at the bed, dye tracing techniques, etc.) (Seaberg and others, 1988; Bingham and others, 2005) along with computational modeling (Rada and Schoof, 2018) on various glaciers show that there is strong correlation between the subglacial drainage system and the basal slip of a glacier that facilitates its motion.

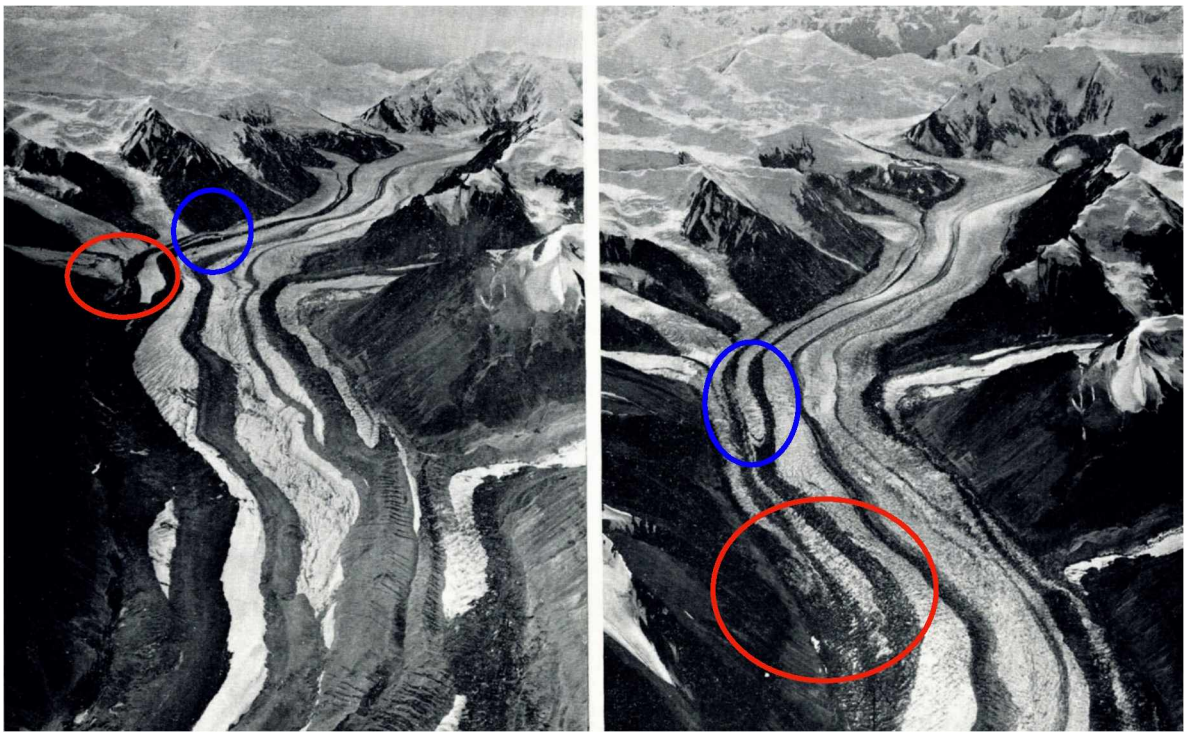

Figure 1.1: This is a repeat photo of the surging Klutlan glacier in the Yukon Territory, Canada. The colored circles show moraine patterns that advance down-glacier. Left: August 1961, around the time when the surge initiated. Right: August 1963, estimated time of the surge termination. Modified and adapted from Post (1969)

1.1 Glacial Water Flow

Glaciers can be regarded as macroporous media because of their capability to capture and distribute water from the surface, which ultimately drains out at the terminus. The main source of water comes from melt that occurs in the *ablation zone*, an area on the glacier surface where melt rates are greater than the annual snowfall. This meltwater can fill cracks on the surface which causes them to fracture through the ice, creating vertical conduits known as *moulins*. These moulins may have direct access to the bed or create englacial passageways, eventually reaching the bed where it is believed that most of the meltwater is transported to(Cuffey and Paterson, 2010).

Other sources of water that have potential connections to the bed are known as *supraglacial lakes*. These lakes are found mostly at the margins of a glacier where ice deforms due to shear stress. Uneven surfaces and depressions form a catchment area that fills with water during the melt season. Lakes can make connections to englacial conduits that lead to the bed (Nye, 1976) and rapidly drain (events like these are known as jökulhlaups) which will locally decouple the glacier from the bed, thus triggering fast ice flow. Events like these have been observed (Armstrong and Anderson, 2020) and modeled (Dow and others, 2015) in 1-D. They are also dependent on the state of the subglacial hydrological system that is active at the bed and on the amount of water supply. Robust mathematical water flow models (Fountain and Walder, 1998; and the references within) show two distinct drainage systems exist: *distributed* and *channelized*.

1.1.1 Distributed Drainage System

A distributed system has flow paths that can be complicated and uniquely morphed (Fig.1.2(b)), covering a relatively large fraction of the glacier bed. The flow of water is also distinct because it travels mainly in transverse directions with respect to the flow of ice. Water travels through carved out portions at the glacier bed known as *cavities* (Kamb, 1987; Fowler, 1987). These cavities are sustained by water present at the bed and the glacier

flowing over bumps at the bed that cause an opening on the lee side of ice flow (Fig.1.3(i,ii)). A system of cavities can have water flowing between them through *orifices*, conduits smaller than the cavities that control the flow of water. Because of the difference in sizes, water will spend more time in cavities than in orifices. Cavities tend to stay open due to the glacier sliding, although if there is an increase in water flux the cavity walls can melt and expand.

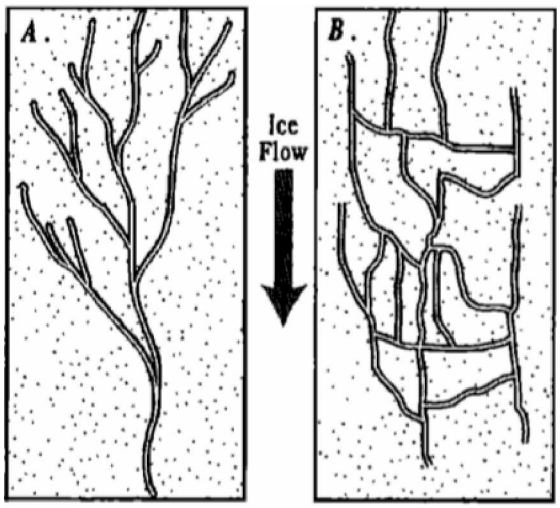

Figure 1.2: Aerial view of (a) channelized and (b) distributed systems at the bed of a glacier. Adapted from Fountain and Walder (1998).

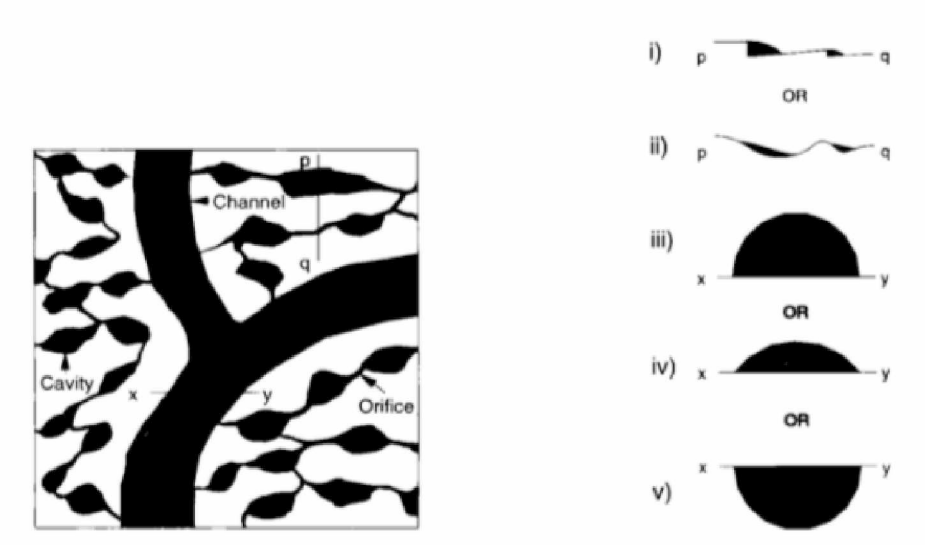

Figure 1.3: Left: Aerial schematic of channels, cavities, and orifices. Right: Cross-sectional areas of cavities (i-ii) and channels (iii-v). Adapted from Willis (1995).

1.1.2 Channelized Drainage System

It is believed that a system of arborescent channels (Fig. 1.2(a)) exists at the bed; many smaller channels coalesce into fewer bigger ones, often resulting in one huge channel that exits at the terminus. These 'R-Channels', as they are commonly known from work by Röthlisberger (1972), have a distinct semi-circular cross-section (Fig.1.3(iii-v)) which can usually be seen at the terminus, but can also have varying cross sectional areas throughout the glacier. The water flowing through the channels melts the walls due to frictional heating, which causes them to expand. With an increase in water flux during the melt season, the channels increase in size which makes a very efficient system in discharging water from the bed.

Incidentally, when channels expand, they lower in water pressure which contrasts with how fluid flows conventionally through pipes. These ice channels act as deformable pipes and change in size depending on the flux of water and the difference in pressures between water and ice. The paths the channels take are determined by a gradient in the water pressure; water flowing through the ice seeks out spaces at lower pressures. Adjacent channels that are smaller will be at a higher water pressure and hence lose water into the larger channels. When there is very little to no water presence in the channels, the glacier's viscous fluid behavior called *creep* takes over which is a slow, continuous deformation of the ice due to the enormous ice pressure brought on by gravity that closes the channels.

1.1.3 Seasonal Evolution of the Drainage Systems

The subglacial drainage systems are driven by melt on the surface which changes seasonally. During the winter, the storage characteristics of the glacier has water present at the base which can move through a cavity system. As spring arrives, more water finds its way to the bed and causes the cavity system to reach a critical profile that cannot handle high water pressures. The cavities transition into channels where their size and water pressure reflects the balance between expansion and closure by creep. Channels preferentially form at

the lowest part of the glacier and continue their formation up-glacier. Glacier motion may increase between the transitions in systems because of the initial increase in water pressure. The channelized system leads to a drop in water pressures and a decrease in speed. When it gets colder, the melt rates start to drop and channels start to shrink. It should be noted that these systems can coexist, depending on the time of the season and basal conditions, and they depend on each other. These structures are also not static and can change in response to the glacier moving.

1.1.4 Water Flow Affecting Basal Slip

With the help of flowing water through advection, heat is supplied and the ice melts causing the glacier to slip easily down the inclined bed. This distribution of water keeps the ice at the bed close to the pressure melting point. Geothermal sources can also supply heat that affects the melting of the ice. As stated before, bumps and ledges at the bed form cavities in the ice and since basal topography does not change significantly in relative short time scales, this makes it possible to always have water present which enhances glacier movement. This is mainly driven by the difference in water and ice pressures, which is also known as the *effective pressure*.

1.2 Black Rapids Glacier (Dału'itsaa'den)

This work is based on investigating a section of the Black Rapids Glacier (BRG) [Ahtna Athabascan name: Dału'itsaa'den - "Where glaciers block off area"], a 40 km long surge-type glacier located in the Eastern Alaska Range (Fig.1.4). It last surged in 1936-1937 and is now in a quiescent phase, although according to mass balance records and forecasting models (Kienholz and others, 2017), it will not surge anytime soon. The BRG lies on a $\sim 2.3°$ slope, and on the Denali Fault, which was subject to a 7.9 magnitude earthquake in 2002 when rockslide deposits covered the lower ablation area. The BRG has been a subject of many research campaigns for the last 50 years, which have revealed things such as a layer of till at

the bed (Truffer and others, 2000) and unusual motion patterns (Fatland and others, 2003) that may be due to the unknown water storage capability under the ice.

For this work, the specific area of interest is located on the main branch of the glacier and its southern branch, the Loket tributary where GPS stakes around the study area (Fig. 1.5(a)) have shown an increase of surface velocity by an order of magnitude for a couple of days after one of the local lakes drains (Fig. 1.5(b)). Past surges of the glacier were initiated on the main branch. During quiescence, the Loket tributary is the major contributor of ice as evidenced by moraine patterns entering onto the main branch. A lake drainage has a similar effect on flow as a surge: for a few days the main branch speed exceeds that of the Loket, after which the pattern reverses again. The lake-induced speed-up can therefore be considered surrogates for a surge. It is difficult to physically study these hydraulically induced displacements coupled with systems that cannot be directly observed; in order to study these speed-ups, a numerical model has to be implemented.

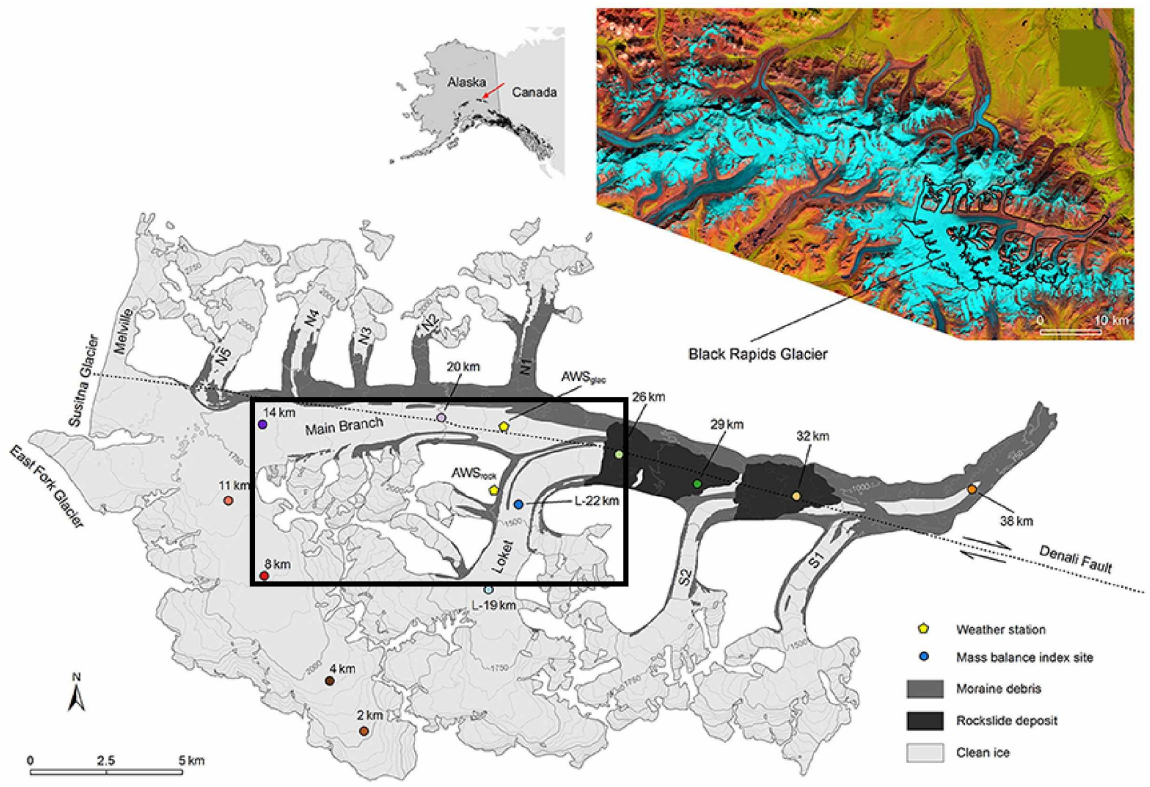

Figure 1.4: Top Left: Geographic map of Alaska pointing towards the Eastern Alaska Range which is pictured in a Landsat false color image, top right. Bottom Half: The BRG map showing the topography, locations of surface instruments, and the debris-laden surface. The rectangular outline is the area of interest. Modified and adapted from Kienholz and others (2017).

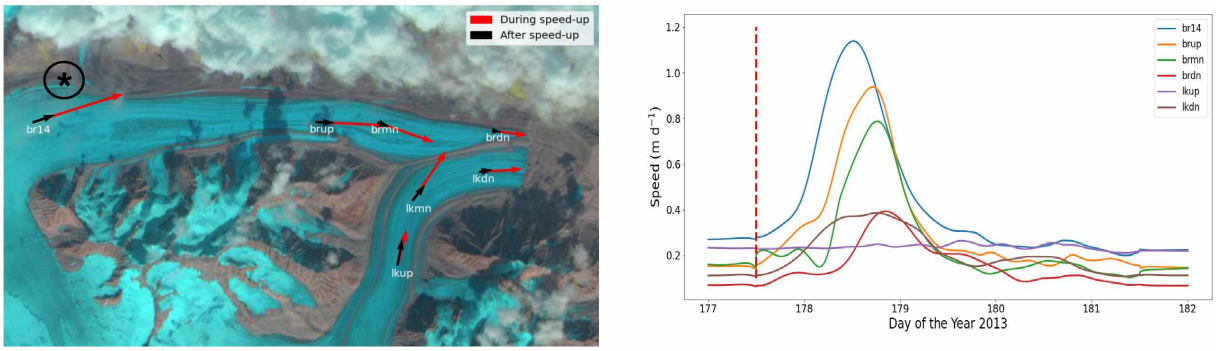

(a) (b)

Figure 1.5: Landsat image of the section of the Black Rapids Glacier that this work focuses on and the GPS stakes on the surface. The circled asterisk is the location of the lake. (b) The surface velocities corresponding to the GPS stakes. The vertical red dashed line is the approximate time of the peak drainage of a local ice-marginal lake.

1.3 Objective

In this work, we use the Glacier Drainage System (GlaDS) model (Werder and others, 2013) to investigate the effects of a lake drainage on the effective pressure distribution beneath the glacier and the tributary. We hypothesize that an increase in basal velocities is reflected in the reduction in effective pressure through an empirical sliding law. We vary the volume of the lake and the times of drainage, both duration and specified dates, to see which has the most influence in speeding up this section of glacier. Physical parameters that directly affect the evolution of both drainage systems are varied to test the sensitivities of the hydraulic conditions at the bed and see whether it weakens or strengthens basal motion. We then compare solutions from a glacier topography with no tributary to see how the confluence contributes to it.

2.0 Model & Methods

2.1 Water Flow at the Glacier Bed

Water flowing at the bed follows a hydraulic potential:

$$\phi = p_w + \rho_w g z \tag{2.1}$$

where p_w is the pressure of water, ρ_w is the density of water, g is the acceleration due to gravity, and z is the elevation of the bed. Along the glacier bed water seeks out spaces with low pressure, so it follows a negative hydraulic gradient:

$$-\nabla\phi = -\nabla p_w - \rho_w g \nabla z \tag{2.2}$$

This gives a general direction of water flow at the bed of the glacier which ultimately leads to the terminus where pressure is the lowest. An important pressure term is the effective pressure, N, defined as the difference between the ice overburden pressure and water pressure:

$$N = p_i - p_w \tag{2.3}$$

where $p_i = \rho_i g H$ is the ice pressure, ρ_i is the ice density, and H is the ice thickness. The effective pressure is relevant for deformation of subglacial till and sliding of ice over its base.

2.1.1 Channelized Model Equations

The derivations for the channel system were first given by Röthlisberger (1972). The assumption is made that there is a steady flow of water in one channel. This gives way to an equilibrium relation that balances melt coming from friction dissipation and water pressure with the expansion of the channel due to melt and closing due to the creep closure from

overburden ice pressure in the following:

$$\underbrace{\left(\frac{d\phi}{ds}\right)^{p+1}}_{\textbf{friction melt}} - \gamma \underbrace{\left(\frac{d\phi}{ds}\right)^{p} \frac{dp_w}{ds}}_{\textbf{pressure melt}} = \zeta \underbrace{Q^{-q} N^{n}}_{\textbf{open/close}} \tag{2.4}$$

Here, ϕ is the hydraulic potential from equation (2.1), s is an oblique spatial dimension that runs parallel to the flow of water, Q is the water flux, γ is a reduction of constants, and ζ is a parameter that represents a mix of constants and ice rheology effects. The exponents p and q are positive numbers that dictate the flow regime of water, either turbulent or laminar. In this case, $p = 3/8$ and $q = 1/4$ because the channel equation (Eq. 2.4) is derived using the Manning formula, which assumes a turbulent flow in a filled pipe and relates the flux to the negative hydraulic potential with a root power: $Q \propto -\sqrt{d\phi/ds}$. The exponent n is known as the *creep exponent* from the shear strain rate power law known as *Glen's Law* which is usually $n = 3$ for ice flow (Fountain and Walder, 1998). If there is no local inclination it follows from Eq. 2.2 that $\nabla z = 0$, then $\phi = p_w$ and we get the following:

$$\frac{dp_w}{ds} = \left(\frac{\zeta}{1-\gamma}\right)^{\frac{1}{1+p}} Q^{-\frac{q}{1+p}} N^{\frac{n}{1+p}} \tag{2.5}$$

The ice channel is a deformable pipe, so high water flux can lead to bigger channels which can be accommodated at lower water pressure, contrary to the flow of water through a fixed diameter pipe as mentioned in chapter 1.

2.1.2 Distributed Cavity Model Equations

Initial theoretical work (Kamb, 1987; Nye, 1976) has shown that the flow in the cavities can be described as the following:

$$Q \approx u_b^l \left(\frac{d\phi}{ds}\right)^{1/2} N^{-n} \tag{2.6}$$

where u_b is the glacier bed sliding speed and l is a positive value that determines the water flow regime. We can assume no inclination again and have $\phi = p_w$, which shows that with an increase in flux, water pressures and basal speeds also increase, but effective pressures decrease. When the water pressure matches the ice pressure, the cavity system becomes unstable (i.e. $1/N \to \infty$.) One thing to note is that the water flux is an increasing function of water pressure unlike in the channels, so when there are two neighboring cavities with a difference in water pressures and size, the larger one with the highest pressure will not lose water to the smaller one.

2.2 Glacier Drainage System (GlaDS) Model

This work utilizes a 2-D finite element flow model that couples both subglacial drainage systems, simulating the evolution of channels on an unstructured mesh and a system of averaged linked cavities that are represented as a water sheet. This model is coded in MATLAB and uses various built-in solvers to fully evolve the subglacial drainage systems. To run this model, a glacier outline (Fig. 2.1) is needed. For this work, an idealized topography (Fig. 2.1(a)) is used for the study area, composed of a rectangular "T-intersection" outline, an undulating bed, and an increasing linear surface profile. An opening is left on the boundary x = 14 km, where the terminus is located and water can drain out. A triangular mesh is generated from Triangle (Shewchuk, 1996)(Fig. 2.1(b)) which creates a network of elements inside the outline domain (see Fig. 2.2 for context on the following.) A random orientation of *edges* (Γ_j) form the mesh that have the potential to form an unbiased system of channels thereby simulating a realistic representation of what happens at glacier beds. The edges meet at *nodes* (Λ_k), potential entry points of surface melt and exchange of water between edges. Nodes also act as corners of *subdomains* (Ω_i), partitions that represent water sheets which also exchange water with the edges.

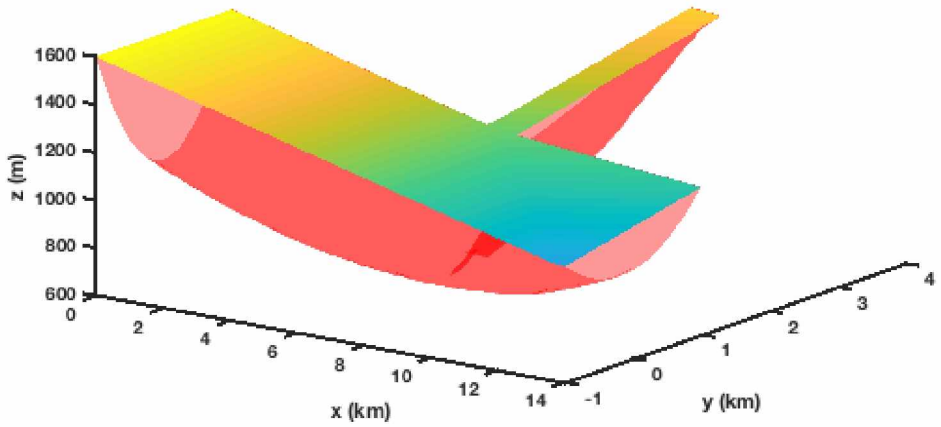

(a)

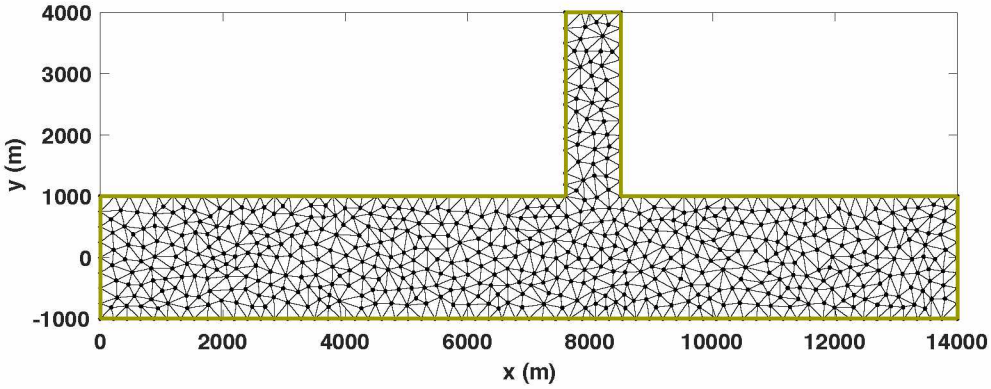

(b)

Figure 2.1: (a) Synthetic glacier outline with the main branch spanning 14 km in length, a 3 km long tributary, a maximum ice thickness of 600 m, and a surface elevation increasing linearly from 1000 m to 1600 m. (b) A triangular, unstructured mesh showing the edges, the nodes, and subdomains surrounded by the glacier outline.

2.2.1 The Model Equations

The numerical model adapts these relations into a set of important equations with the first being the conservation of water mass:

$$\frac{\partial S}{\partial t} + \frac{\partial Q}{\partial s} = \frac{\Xi - \Pi}{\rho_w L_f} + m_c \tag{2.7}$$

where S is the cross-sectional area of a channel, s is the oblique spatial dimension, Q is the water flux (m^3/s), Ξ is the rate of change in potential energy through the channel, Π is the rate of change in sensible heat through the channel, L_f is the latent heat of fusion, and m_c is the source term for the channel for water entering from an adjacent sheet. Water flux is defined as the following:

$$Q(S, \partial\phi/\partial s) = -kS^{\alpha}\left|\frac{\partial\phi}{\partial s}\right|^{\beta-2}\frac{\partial\phi}{\partial s} \tag{2.8}$$

where k is the hydraulic conductivity of water through the channel. The α and β exponents are positive values that are related that dictate the water flow regime, but this parameterization uses the Darcy-Weisbach law which relates the pressure loss in the channel from friction to the average speed of the flowing water (here, α=5/4 and β=3/2 for turbulent flow). The change in size of the channel is controlled by:

$$\frac{\partial S}{\partial t} = \frac{\Xi - \Pi}{\rho_w L_f} - v \tag{2.9}$$

where the first term on the right hand side opens the channel and the second term closes it. The closure rate is due to creep and is given by:

$$v(S, N) = \tilde{A}S|N|^{n-1}N \tag{2.10}$$

where $\tilde{A}$ is an ice rheological flow constant and n is Glen's power law exponent.

A system of linked cavities obeys its unique conservation of mass:

$$\frac{\partial h}{\partial t} + \nabla \cdot \mathbf{q} = m \tag{2.11}$$

where the system can be thought of as a water sheet of variable height h, $\mathbf{q}$ is water flux (m^2/s), and m is the source of water that comes from prescribed melt from the surface and

the bed. Discharge is, again, related to the hydraulic potential:

$$\mathbf{q}(h, \nabla\phi) = -kh^{\alpha}|\nabla\phi|^{\beta-2}\nabla\phi \tag{2.12}$$

The evolution of the water sheet in time is determined by the following:

$$\frac{\partial h}{\partial t} = w - v \tag{2.13}$$

where w and v are the opening and closing terms, respectively. The cavities open with help from the basal speed as follows:

$$w(h) = \begin{cases} u_b \frac{h_r - h}{l_r}, & \text{if } h < h_r \\ 0, & \text{if } h \geq h_r \end{cases} \tag{2.14}$$

where l_r is the length of the horizontal spacing of the water sheet and h_r is vertical spacing, both of which depend on the dimensions of the bumps at the bed. Viscous creep closes the sheet in relation to the effective pressure:

$$v(h, N) = \tilde{A}h|N|^{n-1}N \tag{2.15}$$

which is similar to Eq. 2.8, but here it is formulated in terms of height of the water sheet, rather than cross sectional area.

2.2.2 Boundary Conditions

Solving the drainage systems equations need boundary conditions. In the equations introduced in the previous section, both h and S evolve with respect to time, but ϕ has spatial derivatives that need a prescribed water pressure and water flux. Some edges have a Dirichlet boundary condition, $\phi = \phi_D$, which reflects atmospheric pressure being present where outflow of water occurs (i.e. the terminus.) A Neumann boundary condition, $\partial\phi/\partial n = \Psi_N$, is applied

to prescribe water fluxes:

$$|\mathbf{q}_N| = -kh^{\alpha}\left|\frac{\partial\phi}{\partial s}\right|^{\beta-2}\Psi_N \tag{2.16}$$

which is the inflow of water (moulins/lake) that takes place up-glacier. However, the Neumann boundary condition is usually assigned to be $\Psi_N = 0$ because there is no water input through the glacier boundary. Water enters the system as a source term at specified nodes defined as moulins.

2.2.3 Nodes & Moulins

The nodes in the mesh network act as points of mass conservation where the input of water needs to be accounted for, from surface melt to channels that have water flowing through and meet at the nodes. When receiving discharge from multiple channels, water conservation has to uphold:$\sum_j Q_j^k = 0$, where j channels lead to the k^{th} node. When nodes receive melt from the surface, then the conservation is modified to: $\sum_j Q_j^k = -Q_m^k$, where the m^{th} moulin supplies water into the connected j channels. The amount of water drained through a moulin is calculated from a surface melt parameterization (Sec. 2.3). The sheet and channels are coupled with a water exchange term that preserves mass:

$$m_c = \mathbf{q}\cdot\mathbf{n}|_{\partial\Omega_{i1}} + \mathbf{q}\cdot\mathbf{n}|_{\partial\Omega_{i2}} \tag{2.17}$$

where $\mathbf{n}$ is the direction normal to the channels.

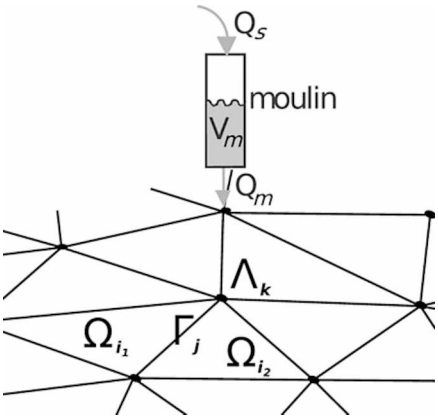

Figure 2.2: A schematic and close look at the mesh showing the edges (Γ_j), nodes (Λ_k), subdomains (Ω_{jl}), the melt water flux (Q_s) flowing into a moulin that fills with a volume (V_m) which delivers a flux (Q_m) to a node. Figure adapted from Werder and others (2013).

2.2.4 Lake Implementation

The lake is modeled as a moulin, but is manually assigned its location on the glacier and the amount of water draining. The draining of the lake is controlled via a function, $L(t)$, that is defined by a asymmetric Gaussian distribution as a function of time:

$$L(t) = \begin{cases} PV \exp(-\frac{(t-t_{PV})^2}{2t_{rl}^2}), & t < t_{PV} \\ PV \exp(-\frac{(t-t_{PV})^2}{2t_{fl}^2}), & t \geq t_{PV} \end{cases} \tag{2.18}$$

PV stands for "peak volume" of the draining lake, t_{PV} is the time the peak volume occurs, t_{rl} is the "rising limb" of the hydrograph or the time it takes to reach the peak volume draining, and t_{fl} is the "falling limb" or the time after the peak drainage. This mimics hydrographs of draining lakes that have appeared in previous works (Nye, 1976; Young, 1980)(Fig. 2.3(a)). The total volume of the lake can be easily found with a simple numerical integration of $L(t)$.

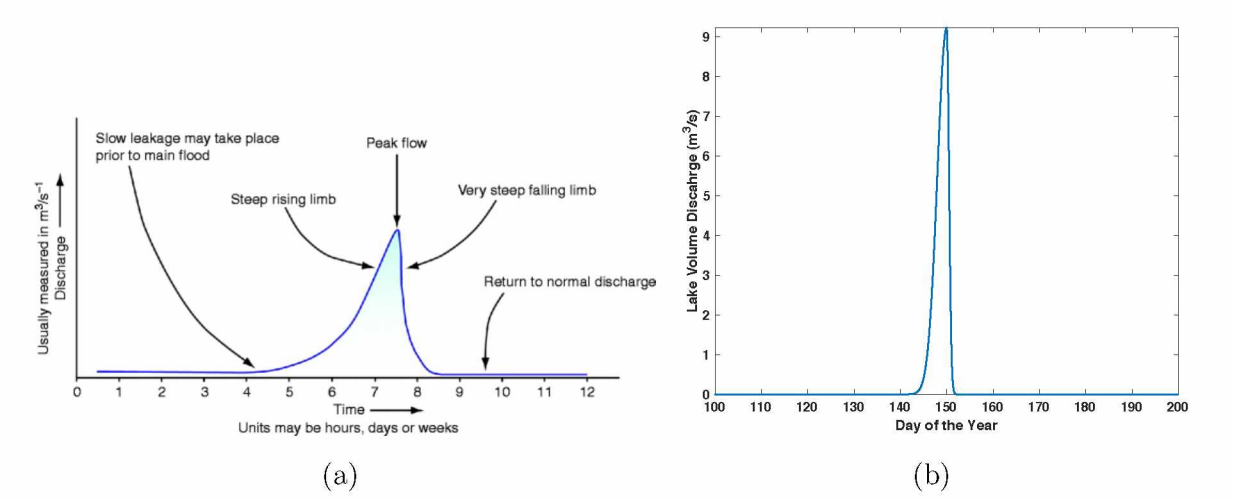

(a) (b)

Figure 2.3: (a) A descriptive lake drainage hydrograph adapted from Young (1980). (b) Example lake hydrograph modeled with Eqn. 2.18.

2.2.5 Numerically Solving the Subglacial Drainage Equations

The idea behind solving the system of drainage equations in section 2.2.1 through a finite element methodology is to consider each local element one at a time. Discrete solutions are needed at these elements in order to satisfy arduous boundary conditions and the cumbersome coupling of ϕ throughout the equations. The way this is dealt with is by writing the drainage equations in their *weak form*. Weak formulation is used to obtain "smooth", approximate solutions from problems that have discontinuities and boundary data that is difficult to deal with in straightforward calculations. We first take a test function (θ is chosen), have it multiply to Eqs.(2.7-2.9) and Eqs.(2.11,2.13), and integrate along the edges and subdomains, respectively. This function is assumed to have the same basis as ϕ, so an acceptable solution can be found. After integrating by parts, we are left with:

$$\begin{aligned}
&\sum_i \int_{\Omega_i} \left[\theta \frac{e_v}{\rho_i g} \frac{\partial \phi}{\partial t} - \nabla\theta \cdot \mathbf{q} + \theta(w - v - m) \right] d\Omega \\
+ &\sum_j \int_{\Gamma_j} \left[-\frac{\partial \theta}{\partial s} Q + \theta \left(\frac{\Xi - \Pi}{L_f} \left(\frac{1}{\rho_i} - \frac{1}{\rho_w} \right) - v_c \right) \right] d\Gamma \\
&+ \int_{\partial\Omega_N} \theta q_N d\Gamma - \sum_k \theta \left(- \frac{A_m^k}{\rho_w g} \frac{\partial \phi}{\partial t} + Q_s^k \right) = 0
\end{aligned} \tag{2.19}$$

Integration by parts cancels out the term that exchanges water between the sheet and channels which maintains an equilibrium pressure. In other words, the sheet and channels will exchange water at any rate to maintain an equal pressure and thus the terms sum up to zero. The sums come from discretizing the system using the *Galerkin method*. This is a useful method because the right choice of test function gives a reasonable residual solution, which in this case is zero. A piecewise linear approach is used to solve Eq. 2.19 at each node. This gives the same number of unknowns and because of the linear approach, the system can be put into matrix form, otherwise known as a *stiffness matrix*. This can be solved using built-in MATLAB solvers and coded time steppers to obtain solutions. This equation (Werder and others, 2013) along with Eqs.(2.9 & 2.13) give the complete model.

2.3 Glacial Melt Water Parameterization

Melt rates vary with elevation on glaciers. When the melt season starts, the rates are greatest at lower elevations and steadily increase up-glacier as it starts to get warmer. This is seen in the following function and in Fig. 2.4:

$$M(H,t) = -(A\cos\omega t)_{>0} + H_s L_r + M_b \tag{2.20}$$

Here A is the amplitude of melt referenced to sea level, t is measured in years, H_s is the surface elevation, L_r is the lapse rate, and M_b is the basal melt factor. To further simulate real-life conditions, the function also has a diurnal component (i.e. the cosine function) where water flow is at a minimum at night and highest during the day. A lower limit of zero is given to this component to ensure that it does not give nonphysical results. The lapse rate is usually a change in temperature with respect to elevation. Here, the lapse rate is chosen as a mass-balance term that reflects the rate of melt per day that decreases with increasing elevation. A rate of -5cm/day/km has been observed (Kienholz and others, 2017) on BRG.

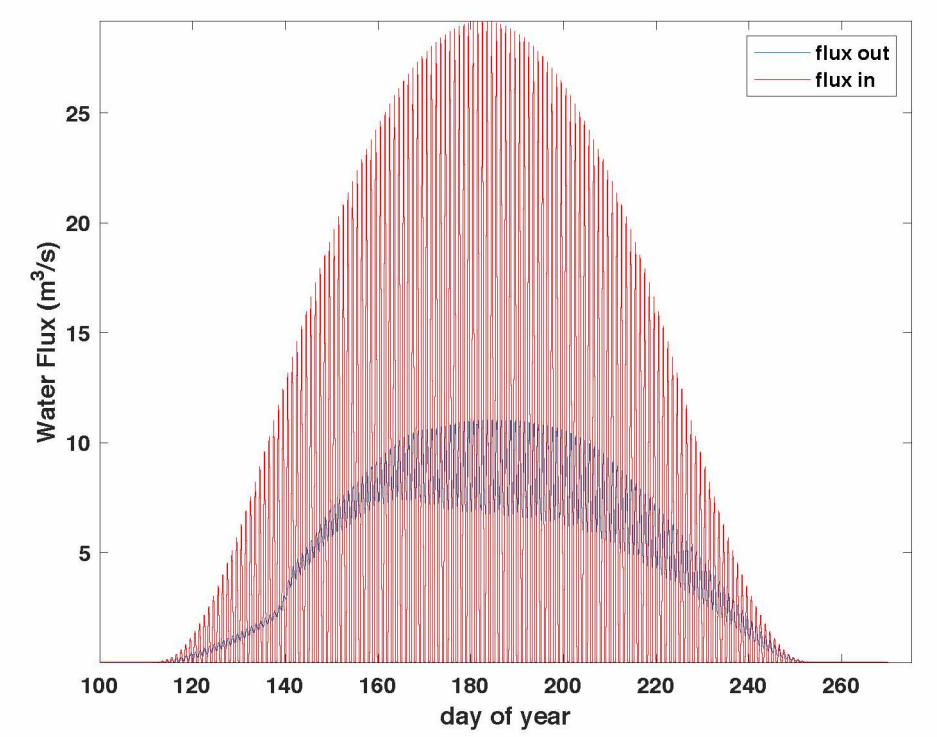

Figure 2.4: The melt factor (Eq.2.20) forcing water (red) into the bed and water exiting out (blue) of the glacier, as calculated by the model. The glacier greatly dampens the large variations in water input.

3.0 Results

All of the following results have been initialized with a spin-up run in order to reduce the dependence on initial conditions. A set of parameters was chosen to simulate observations from the BRG, but the purpose of this work is to investigate the sensitivity of our results with respect to model parameters and forcings that are seen in Table 3.1.

Name	Variable	Units
peak lake volume	PV	m^3/s
cavity spacing	l_r	m
bed bump height	h_r	m
sheet width	l_c	m
time leading to lake drain	t_{rl}	days
time proceeding lake drain	t_{fl}	days
time of peak lake drain	t_{PV}	day

Table 3.1: A table of parameters that are varied in the model runs.

The spin-up run had the following parameter values: $l_r = 2$ m, $h_r = 0.1$ m, $l_c = 2$ m, and no lake assigned. The choice of these values are general to glaciers which have been derived from field work and glaciated valleys (Werder and others, 2013). There are 20 randomly assigned moulins that introduce melt to the bed which will not change throughout the results.

3.1 Lake Drainage

Surface lakes at BRG drain annually, but not always at the same time. The melt seasons can vary in temperatures, so the availability of melt water will also not be the same and lakes can drain very early or late during the season. This also depends on the configuration of the drainage system. In the model, we have the ability to control when and where the lake can

drain. First, we highlight a reference lake drainage with parameters derived from Raymond and Nolan (2000) where they estimated the time and volume of a surface lake draining on the BRG called the Aurora Lake. The peak drainage occurred in mid-June (∼day 134) with a PV of $\sim$ 9.33 m^3/s. The volume of the lake can also be controlled by both the length of the drainage time and peak volume. In the initial lake drain for figures 3.1 and 3.2, we use $t_{rl} = 2$ days, $t_{fl} = 0.5$ day, which gives a total lake volume of $\sim 2.5 \times 10^6$ m^3. The same parameter values were used from the spin-up.

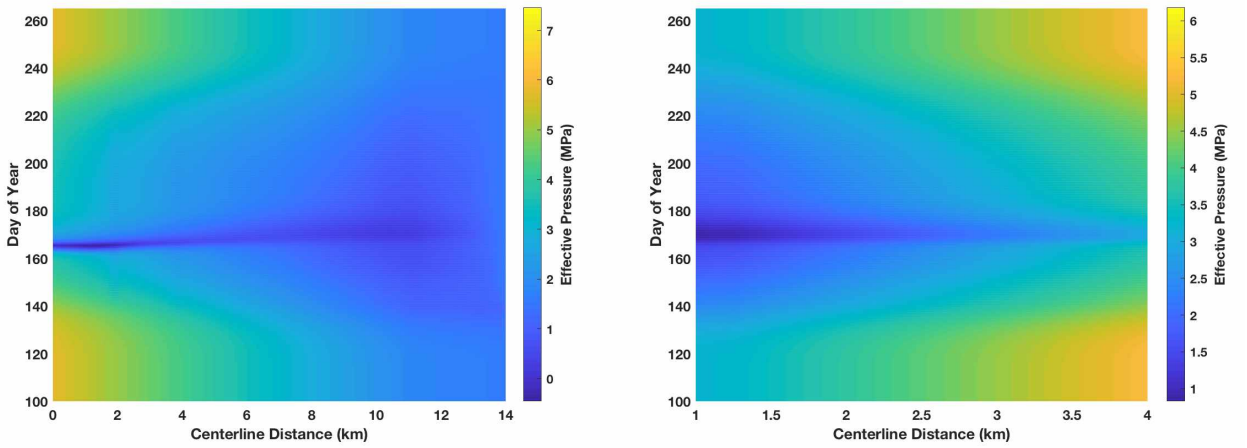

(a) (b)

Figure 3.1: Spatiotemporal maps where the y-axis shows the day of the year, the x-axis is the distance down the center of (a) the main branch and (b) tributary. Color shows effective pressures where low values indicated high water pressure.

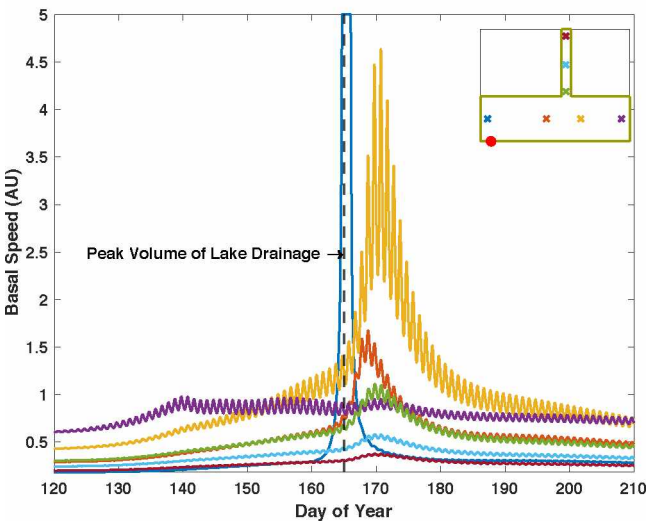

Figure 3.2: Model run of a lake drainage mid-June (day 165, dashed grey line) and the basal speeds around the melt season. The basal speeds are in arbitrary units and the time is noted in days of the year. Each line color represents a centerline position in the inlet map of the glacier. The position of the lake can be seen as the solid red circle.

Change in effective pressure can be seen in Figure 3.1 on both segments of the glacier. This shows that there is a strong subglacial connection between the main branch and tributary. The change in pressure after the drainage progresses down the main branch at a rate of ∼1.45 km/day. We calculate the basal speeds by assuming that they are inversely related to effective pressure by an empirical sliding law (Budd and others, 1979). This law has parameters that are not well constrained. We posit a relation $u_b \propto N^{-1}$ and only use the calculations to examine the timing of the peaks and their relative amplitude at different glacier locations. Because this relation gives unbounded values as $N \to 0$, we prescribe a lower limit of 200 kPa to the effective pressure in order to create an upper bound on derived speeds (Fig. 3.2). The high frequency diurnal nature of Figure 3.2 results from the diurnal effect that drives the melt on the surface.

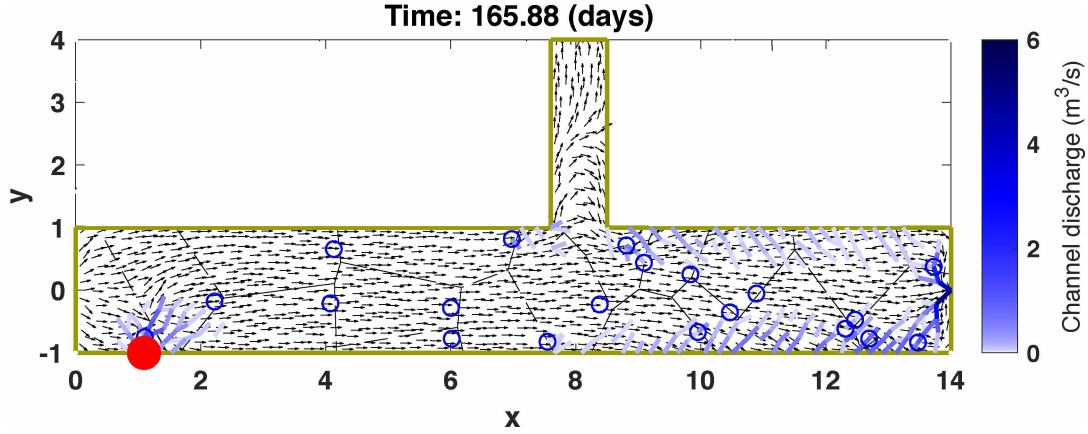

Figure 3.3: Channels form down-glacier and around the lake drainage, although around the lake they formed due to the sudden input of water, but are not sustained due to a lack of steady water input. This plot shows the direction of water flow (black arrows), surface catchment delineations (black dashed lines), moulins and lake (blue circles), draining of water (red circles), and water flux through channels (blue lines) that lead to the terminus (x = 14 km).

A more detailed look at what happens at the bed a day after a lake drainage is seen in Figure 3.3. Around this time, channels form down-glacier as the melt season progresses. The lake has residual water draining which feeds the channel growth, but they will disappear a day or two after the drainage, as water supply terminates.

3.2 Parameter Sensitivity

We vary physical parameters of the glacier bed that are only loosely constrained to investigate sensitivities. We first take a look at the bed bump height, h_r, that was varied from 0.1 m to 4 m, while keeping the remaining parameters constant. Taking a look at Figure 3.4 shows that changing the bump height by an order of magnitude will cause a constant effective pressure. This is due to the large amount of space for water to move beneath the glacier. A lake drainage shows very little effect in basal speeds. For $h_r = 0.5$ m, the speed variations do appear, but they are not as pronounced as for $h_r = 0.1$ m.

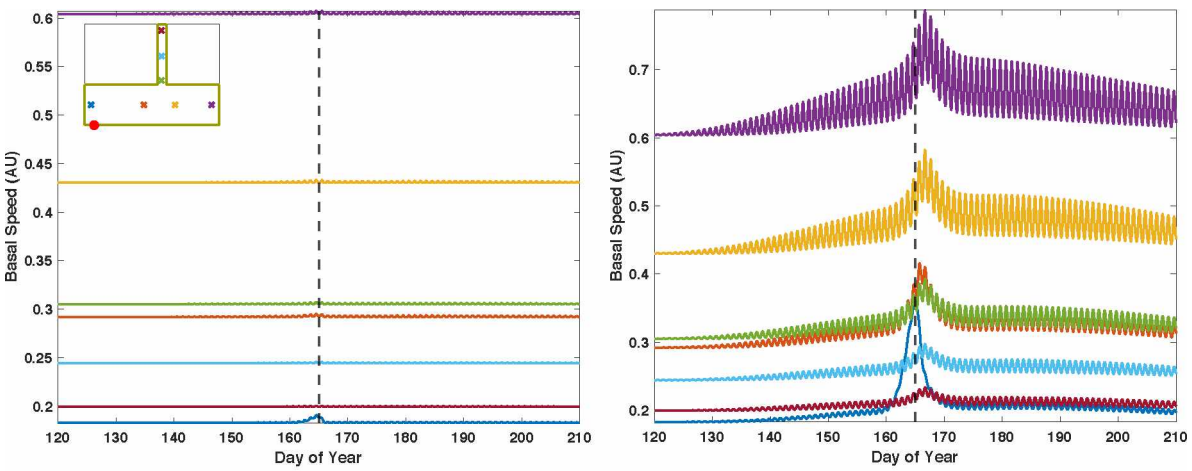

Figure 3.4: (a) Basal speeds are nearly constant with $h_r = 4$ m and (b) $h_r = 0.5$ m has an increase in basal speeds from (a) which shows the importance the ice contact needs to the bed in order for the glacier to speed up.

Next we investigate the effects of decreasing the cavity spacing, l_r, from 2 m to 0.5 m. This controls the spacing between the cavities which increases the opening rate of the cavities. Water has more paths to flow through but still makes enough contact throughout the bed to accelerate the glacier as seen in Figure 3.5(a). The surprising detail in this plot is that the speed signal near the lake (blue, in color) is not as intense; it is much lower in magnitude than the signal at the beginning of the tributary (green, in color.) When the sheet width below the channel, l_c, decreases from 2 m to 0.5 m, this limits the size the channel can grow which results in an increase in water pressure. This can be seen in Figure 3.5(b) where the speed signals intensify in comparison to the reference lake drainage.

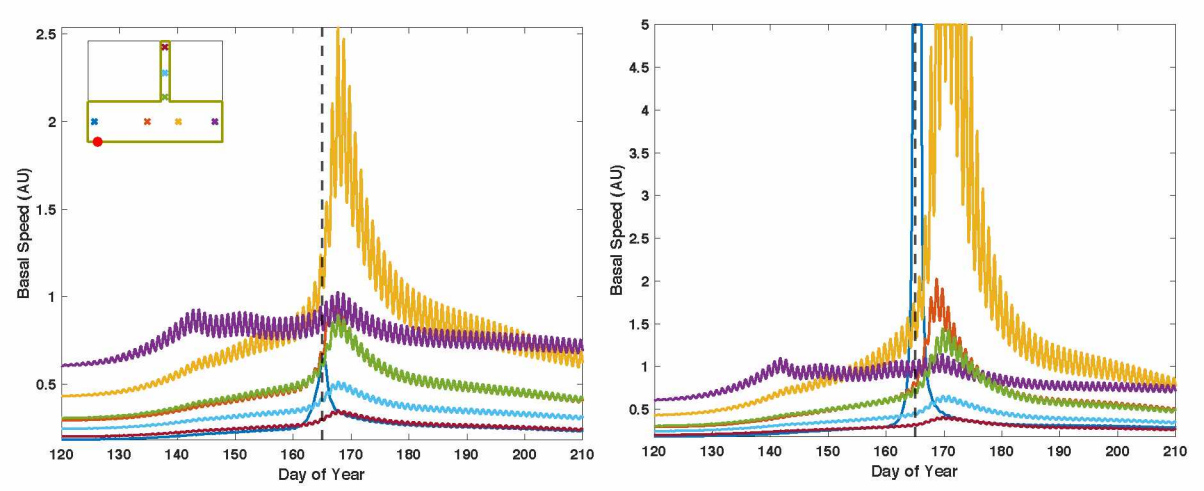

(a) (b)

Figure 3.5: The distributed speeds of the glacier when (a) $l_r = 0.5$ m and (b) $l_c = 0.5$ m. When the cavity spacing is lowered, the water travels through more cavities, but surprisingly makes little impact along the glacier. When the channel width is lowered, speeds intensify slightly more than the reference lake drainage.

3.3 Time and Volume of Lake Drainage

Here we control the duration of the lake drainage and the day in the melt season when it drains. The days of drainage were chosen in the middle of the months during the melt season: mid-May (day 135), mid-June (day 165), and mid-July (day 195). These lake drainage initiation dates were chosen to investigate their effects on a subglacial drainage system in different stages of its seasonal evolution. Studies on supraglacial lake drainage show a hydrograph that is asymmetric, where the start of the drainage lasts longer than the time after the peak volume has been reached. We can test what a symmetric distribution of drainage time does to basal conditions. The following results have the drainage duration with a symmetric time distribution of $t_{rl} = t_{fl} = 3$ days. This extension in lake draining time increases the total lake volume to $6{\times}10^6$ m^3. Comparing the mid-June run (Fig. 3.6(b)) to the reference lake drainage, there is a significant increase in speeds down-glacier. The tracker (green, in color) at the beginning of the tributary shows a large spike in velocity and the trackers following up-tributary show lower speeds, which demonstrates the extent of the lake drainage effects.

In the other dates (Figs. 3.6(a)&(c)) the usual trackers close to the lake reach the upper speed limit while the rest show a residual climb that is not as prominent.

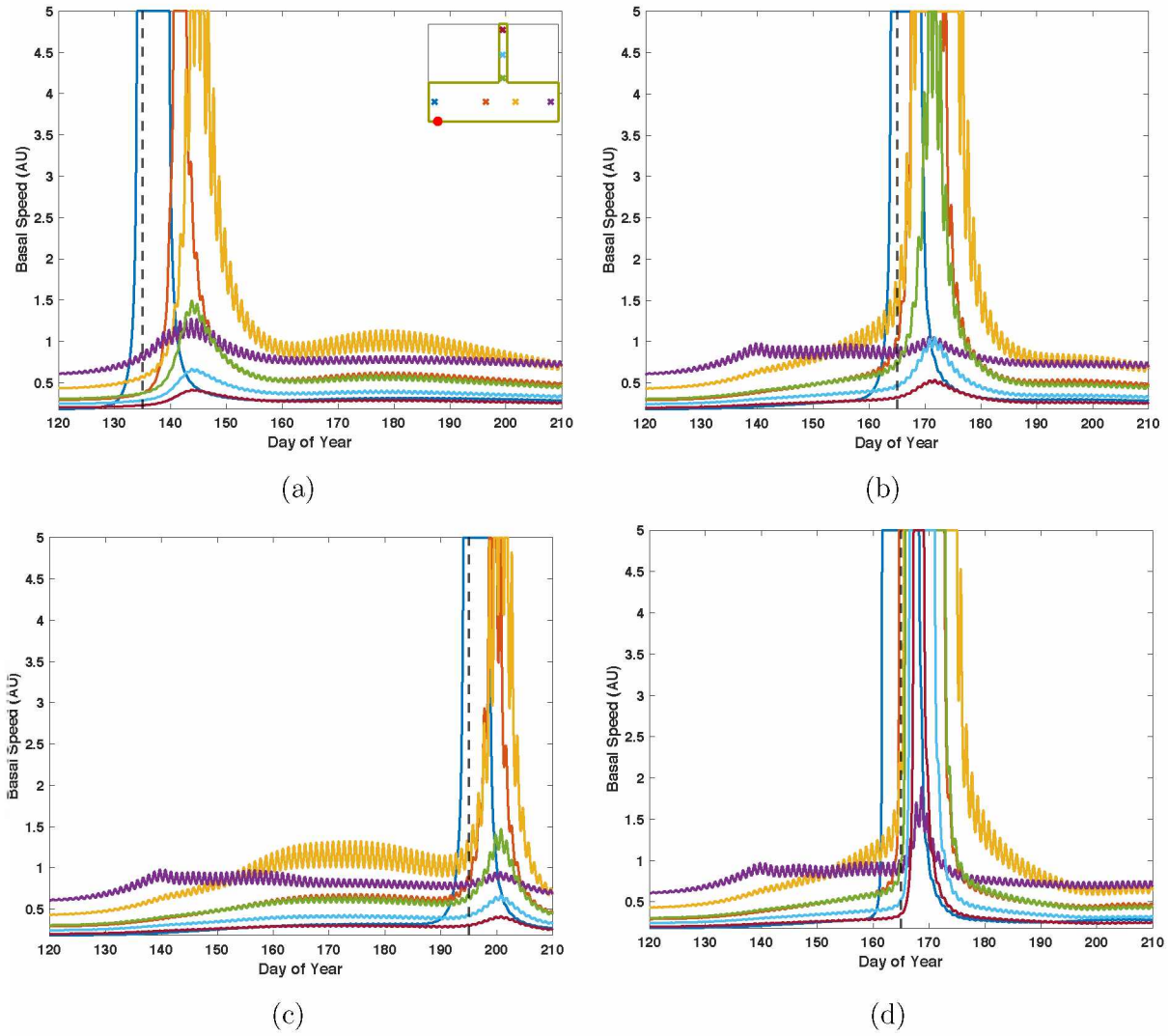

Figure 3.6: Lake draining at different times of the year: (a) mid-May, (b) mid-June, and (c) mid-July. The days surrounding the PV of the lake are symmetric, $t_{rl} = t_{fl} = 3$ days. Figure (d) ($t_{rl} = 2$ days and $t_{fl} = 0.5$ days) shows when the PV is 70 m^3/s, showing a great decrease in effective pressure throughout the bed and a longer duration of a speed-up.

When the PV is increased from 9.22 m^3/s to 70 m^3/s (Fig. 3.6(d)), but with $t_{rl} = 2$ days and $t_{fl} = 0.5$ days, it adds a tremendous amount of water ($\sim 1.9{\times}10^7$ m^3) to the bed and it expands the duration of the drainage. The change in water pressure is so great that it manages to increase the basal speed by the terminus more than a lake draining locally

(See Sec. 3.4), which shows that a channelized system has yet to be established around this time. It could be that any existing channels were too small to handle a large flux of water and it was still part of a distributed drainage system.

3.4 Lake Placement

The lake is placed at locations on or very near the margins where they tend to form. There are three positions on the main branch and one on the tributary that are explored here. The lake is moved down-glacier which makes it susceptible to be connected to a channelized drainage system, because channelization occurs earlier lower down on the glacier. This can be seen in Figure 3.6(b) where only the station nearest the lake experiences a speed-up. The change in flux was not enough to overwhelm the forming channels, in contrast to the results in the previous section. The farther the lake is up-glacier, the more the glacier experiences the change in effective pressure locally, as well as downstream. The most intriguing result in these plots is the persistent signal (yellow, in color) from the location near the intersection. No matter where the lake is drained, or what time of the year, or the volume of the lake drained, it always shows a speed-up.

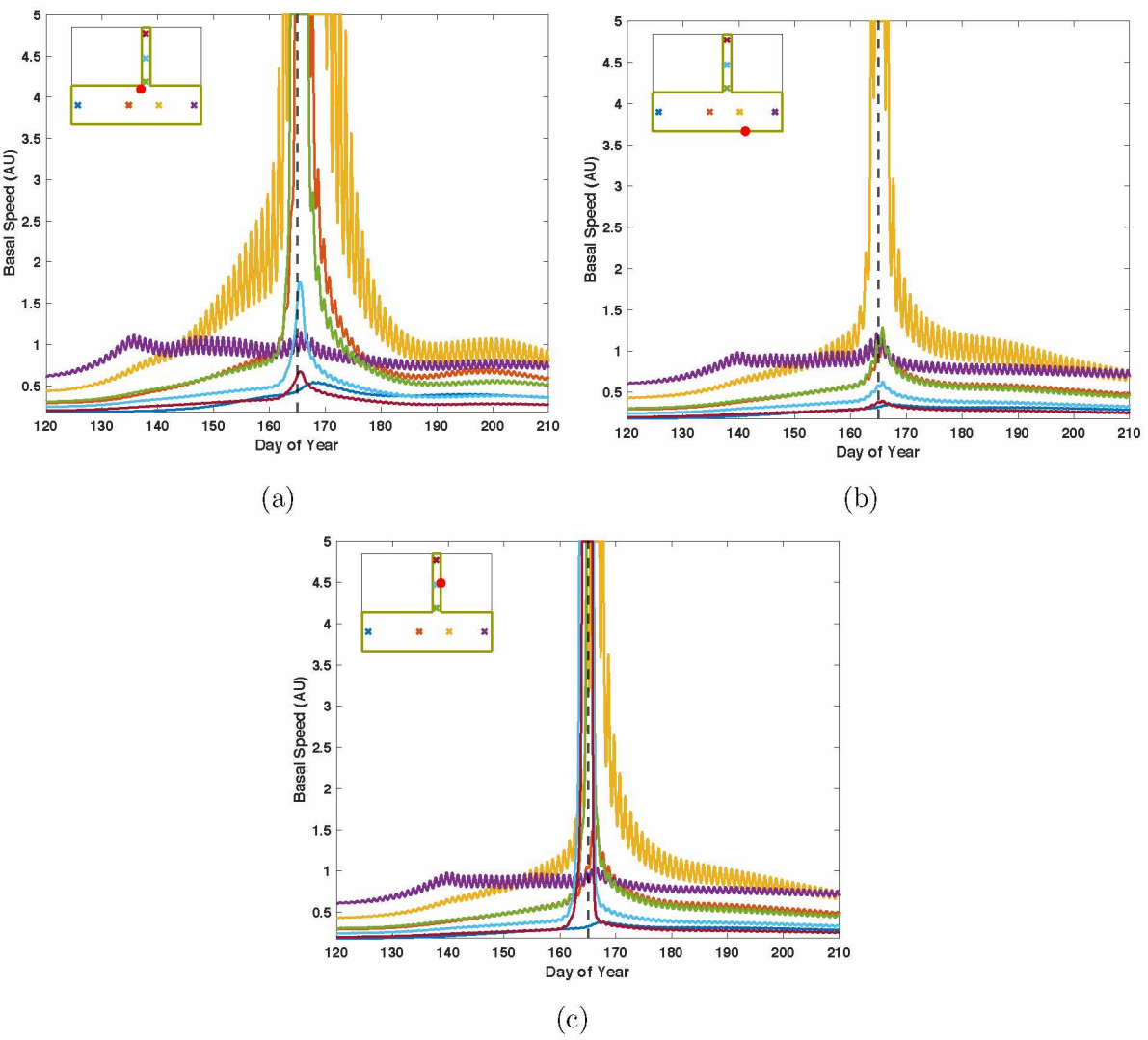

Figure 3.7: Basal speeds of the glacier with a lake draining at different locations: (a) x = 7.48 km, y = 0.83 km, (b) x = 10 km, y = -1 km, and (c) on the tributary (x = 8.5 km, y = 2.5 km).

3.5 Tributary Influence

We further tested the response of a glacier outline without a tributary. In order to show whether the tributary has any influence on the subglacial drainage systems and therefore the motion of the main branch. These model runs use the same parameters and initial conditions as the ones from the reference lake drainage in section 3.1. Results without the tributary show generally lower basal speed signals, especially on the part of the glacier below the tributary intersection. Initially this shows that the tributary contributes a significant

amount of water towards the main branch. We can take a closer look at this by comparing the volume of water coming out of each of the glacier outlines (Fig. 3.9). It seems that there is more water available in an outline with a tributary, for a total volume of 4.4×10^8 m^3, than without a tributary, for a total volume of 3.1×10^8 m^3, with a difference of 1×10^8 m^3. While this model does not track ice flow, it shows that the tributary carries some subglacial hydrological influence onto the main branch.

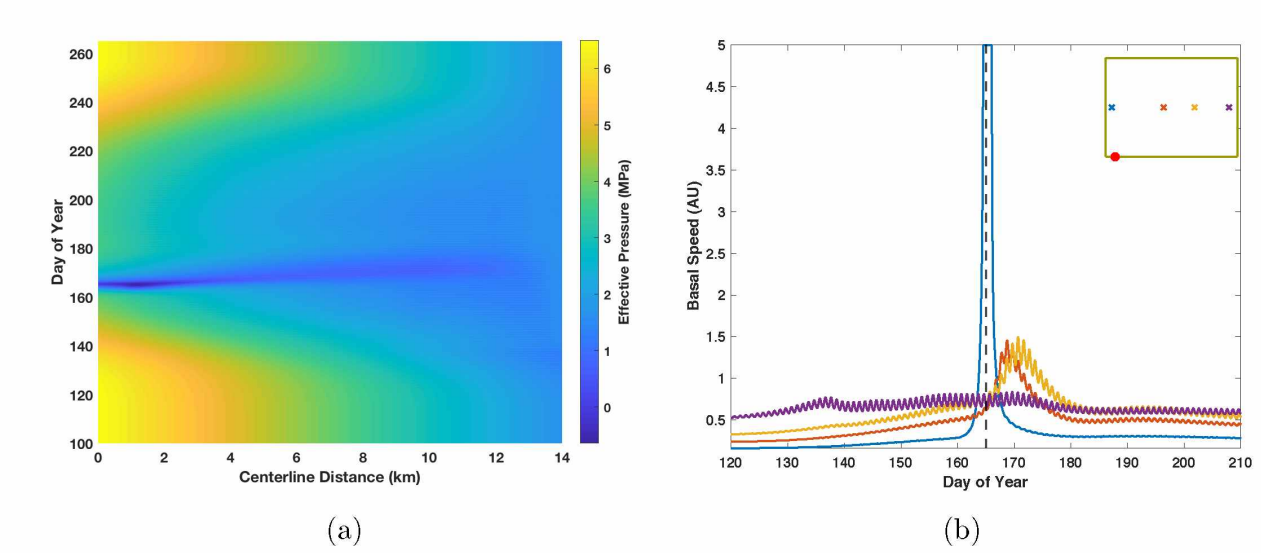

(a) (b)

Figure 3.8: (a) This spatiotemporal map tracks the change in effective pressure underneath the glacier without a tributary. (b) Basal speeds show a dampening of the velocities without a tributary present.

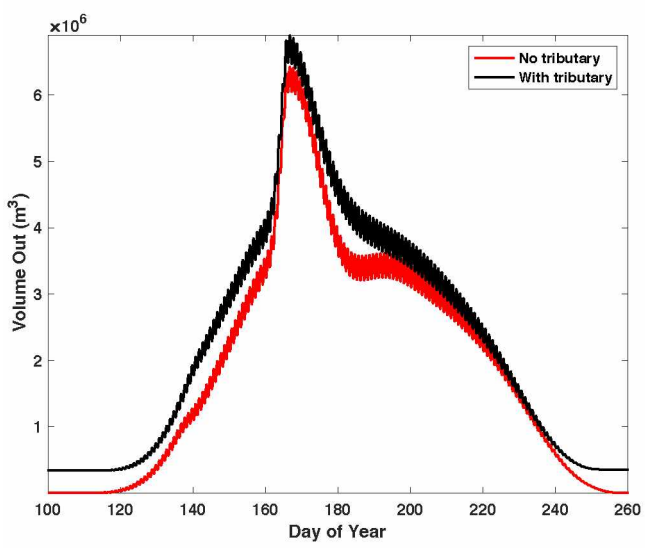

Figure 3.9: A difference in water volumes between glacier outlines with and without a tributary. The steep increase in water draining around day 165 reflects the lake draining for both model runs. There is more water present when a tributary is present.

4.0 Discussion

4.1 Glacier Bed Parameterization

It is noteworthy that all parameters in this study are uniform for the whole glacier, although realistically they can be expected to vary widely throughout an actual glacier. It is thought that there are parts of the bed that are isolated from any drainage system or that they are not connected to the main branch arteries. There also could be a combination of h_r, l_r, and l_c values that give way to efficient water flow, a backup flood of water that causes the glacier to flow faster, or both. This can explain the diversity of storage capacities underneath glaciers (Iken and Truffer, 1997; Harper and others, 2007). The GlaDS model is built on concepts of water flow over bedrock, but it would be interesting to investigate the effects of a layer of till. The BRG is known to have a layer of till at the bed and this can change the water pressures in our results. It is possible that this would lead to higher water pressure, as till is thought to enclose the flow path of water thereby further decreasing values of N (Fountain and Walder, 1998; Truffer and others, 2001).

4.2 Lake Position

Lake position greatly affects the basal speeds of certain sections of glacier. It is seen that a slight decrease in effective pressure reaches up-glacier when the lake is farther down-glacier or on the tributary. Channelization does not reach high elevations, so it shows that a distributed drainage system is mostly active throughout the glacier. This also shows that there may be some drainage backup where water is not being drained efficiently and the sudden input of an enormous amount of water enhances the sliding up-glacier (Armstrong and Anderson, 2020). The location of marginal lakes can be quite random, so it might not be common to find a glacier setting that would have a lake close to the terminus as modeled in this work. However, the results show that lakes could connect to an active channelized system and drain efficiently.

4.3 Lake Volume and Drainage Times

Increasing the duration of the lake drainage time shows that it also increases the water pressure at the bed. However, with a finite volume of water, an actual surface lake may not be capable of supplying more water than it can hold, unless sustained by increasing melt rates and frequent days of precipitation. Also, lake drainage events do not extend more than mere hours of draining because of how efficient it is connected to the glacier plumbing, so to force drainage for more than a day is not reasonable. The lake draining at different stages of the melt season shows different reactions according to the basal speed signals. The strongest change in speeds is shown when the lake drains mid-June (Fig. 3.6(b)) when it is suspected (Rada and Schoof, 2018) that there is a transition between drainage systems that happens which leads to an uptick in basal speeds. This can also be seen by the persistent signal that shows a speed-up around the peak of the melt season which might reflect that transition, but also other factors, such as the tributary feeding meltwater to the main branch, could contribute to the speed-up.

4.4 Tributary Influence

In the model runs with a tributary, velocities on the main branch seem to be amplified by its presence, based on the results without a tributary. It appears that the tributary adds a considerable amount of meltwater. This melt has to be drained through the basal drainage system of the lower main branch. The combined water from melt and from the lake drainage leads to lower effective pressures. It could also be possible that this relation is the key to initiating a surge on the main branch as seen in recent work by Paul and others (2017). They speculate that the slightest advancement of a tributary glacier of the Hispar Glacier, located in the Karakoram in Central Asia, is the cause of its recent surge. With very little superficial evidence on the glacier that would indicate a forthcoming surge, they suspect that a build-up of water pressure due to an inefficient drainage system was at a tipping point that would trigger the surge. It could be that the tributary supplied enough water subglacially that it

started the surge on the main branch. This could be plausible for mini-surges as observed (Kamb and Engelhardt, 1987) on the Variegated Glacier. Water-pressure waves that cause the mini-surges are thought to come from subglacial reservoirs that drain during the melt season. One of the sources of water that is thought to fill the reservoir is the tributary, where bore-hole measurements have shown that areas around the tributary are the origin of the water-pressure waves.

5.0 Conclusion

We have used the 2-D finite element model, GlaDS, to study the effects of draining a marginal supraglacial lake to a glacier bed. A combination of parameters were chosen to simulate a lake drainage that happened on the BRG which became our reference for sensitivity tests to see what inhibits or permits a change in effective pressure underneath our idealized tributary glacier setting. We added a new parameter that represented a lake drainage that models recorded graphs of the water discharge. We then vary the volume of the lake, how long it takes to drain, where it is located, and initial basal conditions,to gain an insight on what helps the acceleration of the glacier.

We found that the cavity opening height over which the glacier flows over has to be relatively small so that there is enough contact with the ice and the bed that the draining water can lubricate the ice and lead to the observed acceleration of the glacier. Otherwise, there is too much space for the water to flow to make an impact on glacier speeds. Decreasing the sheet width underneath the channel shows that it amplifies the speed signals, probably making channel sizes comparable to cavities. This is possible given that the size of channels are not uniform throughout the glacier bed. Changing the time of the lake drainage shows what the state of the drainage system is in the middle of the melt season. Mostly the inefficient system is active throughout the bed because of the speed-up that appears no matter what time in the melt season the lake drainage happens. There are signs of a channelized drainage system when either a lake is placed near the terminus or when all but one speed signal is amplified.

Model runs without a tributary show that there is less water present which results in reduced basal speeds. This suggests that water and the subglacial connection the tributary has with the main branch are key aspects of the tributary contributing to either a surge initiation or a mini-surge. The next step to this model is to add more tributaries, varying their size, elevation, their angle of intersection, etc. It would be particularly interesting

to compare glacier geometries that have tributaries with known melt data and see if this tributary-main branch relation is general for all or just the glaciers that are known to surge.

Modelling the lake draining along with the coupled drainage systems gave us a better insight on a nearly impossible to observe area of a glacier. We did use an ideal case of our study area, but it would be interesting to view these results with an actual outline of the BRG. Temperature is a factor that affects surface melt and lake formation, and this can be used to reflect past records of melt on the BRG and possible mini-surges. The model could also be used to investigate the effect of enhanced melt expected in a warming climate.

References

Armstrong WH and Anderson RS (2020) Ice-marginal lake hydrology and the seasonal dynamical evolution of kennicott glacier, alaska. *Journal of Glaciology*, **66**(259), 699–713

Benn D, Fowler AC, Hewitt I and Sevestre H (2019) A general theory of glacier surges. *Journal of Glaciology*, **65**(253), 701–716

Bingham RG, Nienow PW, Sharp MJ and Boon S (2005) Subglacial drainage processes at a high arctic polythermal valley glacier. *Journal of Glaciology*, **51**(172), 15–24

Budd W, Keage P and Blundy N (1979) Empirical studies of ice sliding. *Journal of glaciology*, **23**(89), 157–170

Cuffey KM and Paterson WSB (2010) *The physics of glaciers*. Academic Press

Dow CF, Kulessa B, Rutt I, Tsai V, Pimentel S, Doyle S, Van As D, Lindbäck K, Pettersson R, Jones G and others (2015) Modeling of subglacial hydrological development following rapid supraglacial lake drainage. *Journal of Geophysical Research: Earth Surface*, **120**(6), 1127–1147

Fatland DR, Lingle CS and Truffer M (2003) A surface motion survey of black rapids glacier, alaska, usa. *Annals of Glaciology*, **36**, 29–36

Fountain AG and Walder JS (1998) Water flow through temperate glaciers. *Reviews of Geophysics*, **36**(3), 299–328

Fowler A (1987) Sliding with cavity formation. *Journal of Glaciology*, **33**(115), 255–267

Harper JT, Humphrey NF, Pfeffer WT and Lazar B (2007) Two modes of accelerated glacier sliding related to water. *Geophysical research letters*, **34**(12)

Harrison WD and Post AS (2003) How much do we really know about glacier surging? *Annals of glaciology*, **36**, 1–6

Hewitt K (2007) Tributary glacier surges: an exceptional concentration at panmah glacier, karakoram himalaya. *Journal of Glaciology*, **53**(181), 181–188

Iken A and Truffer M (1997) The relationship between subglacial water pressure and velocity of findelengletscher, switzerland, during its advance and retreat. *Journal of Glaciology*, **43**(144), 328–338

Kamb B (1987) Glacier surge mechanism based on linked cavity configuration of the basal water conduit system. *Journal of Geophysical Research: Solid Earth*, **92**(B9), 9083–9100

Kamb B and Engelhardt H (1987) Waves of accelerated motion in a glacier approaching surge: the mini-surges of variegated glacier, alaska, usa. *Journal of Glaciology*, **33**(113), 27–46

Kienholz C, Hock R, Truffer M, Bieniek P and Lader R (2017) Mass balance evolution of black rapids glacier, alaska, 1980–2100, and its implications for surge recurrence. *Frontiers in Earth Science*, **5**, 56

Nye J (1976) Water flow in glaciers: jökulhlaups, tunnels and veins. *Journal of Glaciology*, **17**(76), 181–207

Paul F, Strozzi T, Schellenberger T and Kääb A (2017) The 2015 surge of hispar glacier in the karakoram. *Remote Sensing*, **9**(9), 888

Post A (1969) Distribution of surging glaciers in western north america. *Journal of Glaciology*, **8**(53), 229–240

Rada C and Schoof C (2018) Channelized, distributed, and disconnected: subglacial drainage under a valley glacier in the yukon. *The Cryosphere*, **12**(8), 2609–2636

Raymond CF and Nolan M (2000) Drainage of a glacial lake through an ice spillway. *IAHS publication*, 199–210

Röthlisberger H (1972) Water pressure in intra-and subglacial channels. *Journal of Glaciology*, **11**(62), 177–203

Seaberg SZ, Seaberg JZ, Hooke RL and Wiberg DW (1988) Character of the englacial and subglacial drainage system in the lower part of the ablation area of storglaciären, sweden, as revealed by dye-trace studies. *Journal of Glaciology*, **34**(117), 217–227

Sevestre H and Benn DI (2015) Climatic and geometric controls on the global distribution of surge-type glaciers: implications for a unifying model of surging. *Journal of Glaciology*, **61**(228), 646–662

Shewchuk JR (1996) Triangle: Engineering a 2d quality mesh generator and delaunay triangulator. In *Workshop on Applied Computational Geometry*, 203–222, Springer

Truffer M, Harrison WD and Echelmeyer KA (2000) Glacier motion dominated by processes deep in underlying till. *Journal of Glaciology*, **46**(153), 213–221

Truffer M, Echelmeyer KA and Harrison WD (2001) Implications of till deformation on glacier dynamics. *Journal of Glaciology*, **47**(156), 123–134

Werder MA, Hewitt IJ, Schoof CG and Flowers GE (2013) Modeling channelized and distributed subglacial drainage in two dimensions. *Journal of Geophysical Research: Earth Surface*, **118**(4), 2140–2158

Willis IC (1995) Intra-annual variations in glacier motion: a review. *Progress in Physical Geography*, **19**(1), 61–106

Young G (1980) Monitoring glacier outburst floods. *Hydrology Research*, **11**(5), 285–300